Directional Dicke Subradiance with Nonclassical and Classical Light Sources

Daniel Bhatti,[1,2,*] Raimund Schneider,[1,2] Steffen Oppel,[1] and Joachim von Zanthier[1,2]
[1]Institut für Optik, Information und Photonik, Universität Erlangen-Nürnberg, 91058 Erlangen, Germany
[2]Erlangen Graduate School in Advanced Optical Technologies (SAOT), Universität Erlangen-Nürnberg, 91052 Erlangen, Germany

(Received 27 November 2017; published 16 March 2018)

We investigate Dicke subradiance of $N \geq 2$ distant quantum sources in free space, i.e., the spatial emission patterns of spontaneously radiating noninteracting multilevel atoms or multiphoton sources, prepared in totally antisymmetric states. We find that the radiated intensity is marked by a full suppression of spontaneous emission in particular directions. In resemblance to the analogous, yet inverted, superradiant emission profiles of N distant two-level atoms prepared in symmetric Dicke states, we call the corresponding emission patterns *directional Dicke subradiance*. We further derive that higher-order intensity correlations of the light emitted by statistically independent thermal light sources display the same directional Dicke subradiant behavior and show that it stems from the same interference phenomenon as in the case of quantum sources. We finally present measurements of directional Dicke subradiance for $N = 2, \ldots, 5$ distant thermal light sources corroborating the theoretical findings.

DOI: 10.1103/PhysRevLett.120.113603

Dicke superradiance, i.e., the enhanced spontaneous emission in space and time of atoms in highly entangled symmetric Dicke states, has been extensively studied over the last 60 years [1–16]. The corresponding directional emission of spontaneous radiation has been exploited in various quantum communication protocols [17–23] and, more recently, also in the newly evolving field of chiral quantum optics [24–27]. By contrast, its cryptic twin, subradiance, has been much less investigated, mainly due to its higher degree of complexity and increased demands for experimental verification, even though considerable progress has been made recently. Since the first indirect observation [28], the main focus has been on studying the subradiance of two two-level atoms [29–33]. This configuration is most transparent, less fragile [34], and, moreover, can be prepared in both parities, a fully symmetric as well as a fully antisymmetric state, where the latter decouples entirely from the vacuum field for small atom separations [4,5]. Yet, for $N > 2$ two-level atoms, the subradiant Dicke states are merely nonsymmetric [1]; the corresponding states have recently been used to form a unimodular basis [35,36]. Various theoretical investigations have discussed the preparation [9,37–49], as well as the subradiant emission characteristics, of nonsymmetric Dicke states for such larger atomic ensembles, either using a semiclassical theory [9,43–49] or within a full quantum mechanical treatment [13,40–42]. Very recently, the first experimental observation of retarded subradiant spontaneous decay for $N > 2$ emitters was reported [50].

Most theoretical studies of subradiant systems have investigated the temporal aspects of subradiance, whereas only a few have been devoted to its particular spatial emission properties [13,40,43]. Yet, in correspondence to their superradiant counterparts, distant sources prepared in fully antisymmetric states—thus far investigated only for $N = 2$ particles—or nonsymmetric Dicke states display pronounced directional emission profiles, e.g., exhibiting a strong suppression of spontaneous radiation in particular directions [13].

In this Letter, we examine what we call *directional Dicke subradiance*, i.e., the spatial emission characteristics of $N \geq 2$ distant light sources arranged in totally antisymmetric states, enabling the complete suppression of radiation in distinct directions, thereby contributing to the long ongoing study of the manipulation of spontaneous decay. We start to analyze the conditions for achieving totally antisymmetric Dicke states for $N \geq 2$ multilevel atoms or multiphoton quantum sources and explore the specific spatial emission profiles of quantum emitters prepared in such states. We thereafter discuss the possibilities of observing subradiant directional emission behavior of classical sources. Specifically, we show that the same photon interferences and thus the same subradiant suppression of incoherent radiation derived for quantum emitters can be obtained with thermal light sources (TLS) if projected into particular correlated states via photon detection. Finally, we present measurements of directional Dicke subradiance for up to five TLS.

In general, a totally antisymmetric state of N sources is defined by

$$|A_N\rangle = \frac{1}{\sqrt{N!}} \sum_{\mathcal{P}} \mathrm{sgn}(\mathcal{P}) |n_{\mathcal{P}_1}, n_{\mathcal{P}_2}, \ldots, n_{\mathcal{P}_N}\rangle, \qquad (1)$$

where $|n_{\mathcal{P}_l}\rangle$ describes the state of source l, where $l = 1, \ldots, N$, and $\sum_{\mathcal{P}}$ represents the sum over all permutations of

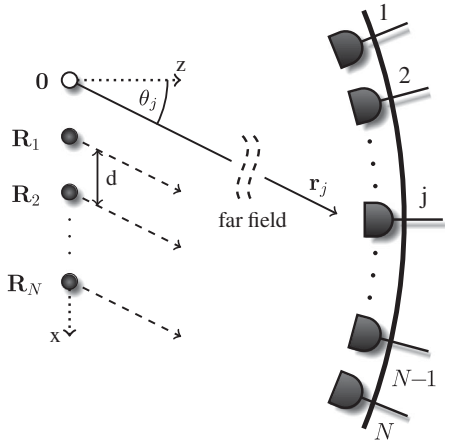

FIG. 1. Setup considered for the oberservation of directional Dicke subradiance: N light sources are aligned along the x axis equidistantly at positions $\mathbf{R}_l$, $l = 1, \ldots, N$, with separation $d \gg \lambda$. In the far field of the sources, N detectors measure the Nth-order correlation function at positions $\mathbf{r}_j$, $j = 1, \ldots, N$.

the entries $\{n_1, \ldots, n_N\}$, with $\mathrm{sgn}(\mathcal{P})$ being the sign of the permutation. According to Eq. (1), in order to realize a totally antisymmetric state, all sources have to be prepared in distinct states, i.e., $n_i \neq n_j$, for $i \neq j$; otherwise, the state vanishes. Specifically, in the case of two-level atoms, a fully antisymmetric state only exists for $N = 2$ particles. Thus, constructing totally antisymmetric states for $N > 2$ emitters requires internal level schemes with at least N distinguishable states, e.g., an excited state $|e\rangle$ and $N-1$ distinguishable ground states $|g_{\tilde{l}}\rangle$, $\tilde{l} = 1, \ldots, N-1$ [48]. We call this kind of source a *multilevel single photon emitter* (MSPE). To construct a totally antisymmetric state for N MSPEs, we can choose for example $n_1 = e$, $n_2 = g_1$, $n_3 = g_2, \ldots$, and $n_N = g_{N-1}$.

To determine the spatial emission characteristics of such a state, we assume without loss of generality the simple source arrangement shown in Fig. 1, where N MSPEs are located equidistantly, with separation $d \gg \lambda$ along the x axis at positions $\mathbf{R}_l = ld\mathbf{e}_x$, $l = 1, \ldots, N$. The intensity recorded at position $\mathbf{r}_1$ is defined by

$$I(\mathbf{r}_1) = G^{(1)}_{\rho}(\mathbf{r}_1) = \langle E^{(-)}(\mathbf{r}_1) E^{(+)}(\mathbf{r}_1) \rangle_{\rho}, \tag{2}$$

where ρ is the density matrix of the N MSPEs, and the (dimensionless) positive frequency part of the electric field operator in the far field of the sources is given by [15]

$$[E^{(-)}(\mathbf{r}_1)]^{\dagger} = E^{(+)}(\mathbf{r}_1) \propto \sum_{l=1}^{N} e^{-il\delta_1} \hat{S}^{(l)}_{-}. \tag{3}$$

In Eq. (3), $l\delta_1 = -lkd\sin(\theta_1)$ corresponds to the relative phase of a photon emitted by source l and recorded by a detector at $\mathbf{r}_1$ with respect to a photon emitted at the origin (see Fig. 1), and $\hat{S}^{(l)}_{-} = (1/\sqrt{N-1}) \sum_{\tilde{l}=1}^{N-1} \hat{s}^{(l,\tilde{l})}_{-}$ is the sum over all atomic lowering operators $\hat{s}^{(l,\tilde{l})}_{-} = |g_{\tilde{l}}\rangle_l \langle e|$, $\tilde{l} = 1, \ldots, N-1$, deexciting the lth MSPE from its upper state $|e\rangle_l$ to the ground state $|g_{\tilde{l}}\rangle_l$.

For N MSPEs in the antisymmetric state $|A_N\rangle$ with one excitation, i.e., with $\sum_{l=1}^{N} \langle \hat{S}^{(l)}_{+} \hat{S}^{(l)}_{-} \rangle_{|A_N\rangle} = 1$, the intensity as a function of δ_1 calculates to

$$\begin{aligned} I_{|A_N\rangle}(\delta_1) &= \langle A_N | E^{(-)}(\mathbf{r}_1) E^{(+)}(\mathbf{r}_1) | A_N \rangle \\ &= \sum_{l=1}^{N} \langle \hat{S}^{(l)}_{+} \hat{S}^{(l)}_{-} \rangle_{|A_N\rangle} + \sum_{\substack{l_1, l_2 = 1 \\ l_1 \neq l_2}}^{N} e^{i\delta_1 (l_1 - l_2)} \langle \hat{S}^{(l_1)}_{+} \hat{S}^{(l_2)}_{-} \rangle_{|A_N\rangle} \\ &= \frac{N}{N-1} \left(1 - \frac{1}{N^2} \frac{\sin(\frac{N\delta_1}{2})^2}{\sin(\frac{\delta_1}{2})^2} \right), \end{aligned} \tag{4}$$

where in the second line of Eq. (4) all interference terms contribute with equal weight, $\langle \hat{S}^{(l_1)}_{+} \hat{S}^{(l_2)}_{-} \rangle_{|A_N\rangle} = -1/[N(N-1)]$, for $l_1 \neq l_2$. More specifically, in Eq. (4) the interference term arises from the fact that all possible combinations of two sources interfere with each other since the single excitation is equally shared among all sources [see Eq. (1)]. This is basically identical to the concept of superradiance arising from symmetric Dicke states (see, e.g., Refs. [13–16]), with the difference, however, that here the antisymmetry of the state introduces a negative sign in front of all interference terms of two distinct sources $l_1 \neq l_2$. In contrast to the emission enhancement of superradiance, the negative correlation between the sources leads to complete destructive interference and thus to a complete suppression of emission in certain directions. Note that the equal negative correlation is also displayed by the cross-correlation coefficient [51], which is identical for all source pairs $l_1 \neq l_2$, i.e.,

$$\frac{\langle \hat{S}^{(l_1)}_{+} \hat{S}^{(l_2)}_{-} \rangle_{|A_N\rangle}}{\sqrt{\langle \hat{S}^{(l_1)}_{+} \hat{S}^{(l_1)}_{-} \rangle_{|A_N\rangle} \langle \hat{S}^{(l_2)}_{+} \hat{S}^{(l_2)}_{-} \rangle_{|A_N\rangle}}} = -\frac{1}{N-1}. \tag{5}$$

In more detail, Eq. (4) displays an intensity profile marked by pronounced dips of vanishing radiation, analogous, yet inverted, to the intensity profile of N two-level atoms in *symmetric* Dicke states, arranged in the same manner as in Fig. 1 [13]. A *superradiant* emission profile can, furthermore, be observed when recording higher-order intensity correlation functions for both N uncorrelated fully excited two-level atoms [14,15] and N uncorrelated classical light sources [14,16]. Yet, in contrast to the sharp peaks of *increased* intensity in the case of superradiant emission, the inverted grating function of Eq. (4) reveals highly focused dips of *reduced* intensity, i.e., directional Dicke subradiance. Equal to its superradiant counterpart [13–16], the subradiant intensity profile of Eq. (4) for N MSPEs in the antisymmetric state $|A_N\rangle$ with one excitation displays a visibility of $\mathcal{V} = 1$, with the minima located at

$\delta_1 = 2m\pi$, $m \in \mathbb{Z}$, having an angular width of $\delta\theta_1 \approx 2\pi/(Nkd)$. These properties describe distinctive features of superradiance [13–16] but can also be used, as in our case, to characterize the particular attributes of Dicke subradiance.

A further option to construct totally antisymmetric states $|A_N\rangle$ and observe the corresponding subradiant behavior is to make use of multiphoton sources (MPSs). Hereby, each source l emits a discrete number of photons n_l, assumed to be different from the other sources, i.e., $n_i \neq n_j$, for $i \neq j$. This could be realized, e.g., by combining n_l single photon emitters for each source l. Again considering the source arrangement of Fig. 1, the (dimensionless) positive frequency part of the electric field operator in the far field of the sources reads [16]

$$[E^{(-)}(\mathbf{r}_1)]^\dagger = E^{(+)}(\mathbf{r}_1) \propto \sum_{l=1}^{N} e^{-il\delta_1}\hat{a}_l, \tag{6}$$

where $\hat{a}_l$ denotes the annihilation operator of a photon emitted from the lth MPS. Choosing $n_1 = 0$, $n_2 = 1, \ldots, n_N = N-1$ again yields the intensity profile of Eq. (4), i.e., a distribution following a negative grating function and displaying directional Dicke subradiance, yet with a different global prefactor of $N^2/2$ [52].

Note that when computing the Nth-order intensity correlation function $G^{(N)}_{N\mathrm{TLS}}(\delta_1, \ldots, \delta_N)$ of a light field produced by N TLS, similar multiphoton interference terms appear as those occurring in the derivation of $I_{|A_N\rangle}(\delta_1)$ for N MPSs [52]. This indicates how directional subradiant behavior can also be observed with classical light sources, i.e., by exploiting correlations produced among TLS when recording a specific number of photons at particular positions [14,16].

To corroborate this argument, we consider again the source arrangement of Fig. 1, where this time N detectors are placed at positions $\mathbf{r}_j$, $j = 1, \ldots, N$, in the far field of N TLS. The density matrix $\rho_{N\mathrm{TLS}}$ of the field generated by the N TLS can be written in the number-state representation in the form [14,16]

$$\rho_{N\mathrm{TLS}} = \bigotimes_{l=1}^{N} \sum_{n_l=0}^{\infty} P_{\mathrm{TLS}}(n_l)|n_l\rangle\langle n_l|, \tag{7}$$

where $P_{\mathrm{TLS}}(n_l)$ denotes the (Bose-Einstein) distribution of source l, and we assume equal mean photon numbers for all sources, i.e., $\bar{n} = \bar{n}_l = \langle \hat{a}_l^\dagger \hat{a}_l \rangle_\rho$, $l = 1, \ldots, N$.

The Nth-order intensity correlation function for N light sources is defined by [53]

$$G^{(N)}_N(\mathbf{r}_1, \ldots, \mathbf{r}_N) = \left\langle : \prod_{j=1}^{N} E^{(-)}(\mathbf{r}_j)E^{(+)}(\mathbf{r}_j) : \right\rangle_{\rho_N}, \tag{8}$$

where $\langle : F : \rangle_{\rho_N}$ represents the (normally ordered) quantum mechanical expectation value of the operator F for a field in the state ρ_N.

To observe directional Dicke subradiance via measurements of $G^{(N)}_N(\mathbf{r}_1, \ldots, \mathbf{r}_N)$, we suppose that $N-1$ detectors are placed at the fixed *subradiant positions* (SP)

$$\delta_j = 2\pi\frac{(j-1)}{N}, \qquad j = 2, \ldots, N. \tag{9}$$

These positions are identical to the arguments of the Nth roots of unity and therefore fulfill the identity

$$\sum_{j=2}^{N} e^{i\delta_j n} = \begin{cases} -1, & n \neq \{0\}, \mod (N) \\ (N-1), & n = \{0\}, \mod (N) \end{cases}. \tag{10}$$

Since we assume N statistically independent TLS, we can make use of the Gaussian moment theorem to also write Eq. (8) in the form

$$G^{(N)}_{N\mathrm{TLS}}(\delta_1, \ldots, \delta_N) = \sum_{\mathcal{P}} \prod_{j=1}^{N} \langle E^{(-)}(\delta_j)E^{(+)}(\delta_{\mathcal{P}_j})\rangle, \tag{11}$$

where $\sum_{\mathcal{P}}$ now refers to the sum over all permutations of the N detectors, and the first moment is given by [see Eq. (6)]

$$\langle E^{(-)}(\delta_{j_1})E^{(+)}(\delta_{j_2})\rangle = \bar{n}\sum_{l=1}^{N} e^{il(\delta_{j_1}-\delta_{j_2})}, \tag{12}$$

where the label $\rho_{N\mathrm{TLS}}$ of the expectation value has been dropped for simplicity.

In the case in which detector δ_1 is not involved in the sum, i.e., for $j_{1/2} = 2, \ldots, N$, Eq. (12) simplifies to [see Eq. (10)]

$$\begin{aligned}\langle E^{(-)}(\delta_{j_1})E^{(+)}(\delta_{j_2})\rangle &= \bar{n}\left(1 + \sum_{l=2}^{N} e^{i\delta_l(j_1-j_2)}\right) \\ &= \begin{cases} 0, & (j_1-j_2) \neq \{0\}, \mod (N) \\ N\bar{n}, & (j_1-j_2) = \{0\}, \mod (N) \end{cases},\end{aligned} \tag{13}$$

which means that all cross-correlation terms for any two fixed detectors $j_1 \neq j_2$ vanish. Equation (11) thus reduces to

$$\begin{aligned}G^{(N)}_{N\mathrm{TLS}}(\delta_1, \mathrm{SP}) = &\prod_{j=1}^{N} \langle E^{(-)}(\delta_j)E^{(+)}(\delta_j)\rangle \\ &+ \sum_{k=2}^{N} |\langle E^{(-)}(\delta_1)E^{(+)}(\delta_k)\rangle|^2 \\ &\times \prod_{\substack{j=2 \\ j\neq k}}^{N} \langle E^{(-)}(\delta_j)E^{(+)}(\delta_j)\rangle,\end{aligned} \tag{14}$$

where the interference term is given by [see Eq. (10)]

$$\sum_{k=2}^{N} |\langle E^{(-)}(\delta_1) E^{(+)}(\delta_k)\rangle|^2 = \sum_{k=2}^{N} \left| \bar{n} \sum_{l=1}^{N} e^{il(\delta_1-\delta_k)} \right|^2$$
$$= \bar{n}^2 (N-1) \sum_{l_1,l_2=1}^{N} e^{i\delta_1(l_1-l_2)}$$
$$- \bar{n}^2 \sum_{\substack{l_1,l_2=1 \\ l_1\neq l_2}}^{N} e^{i\delta_1(l_1-l_2)}$$
$$= \bar{n}^2 N^2 \left(1 - \frac{1}{N^2} \frac{\sin(\frac{N\delta_1}{2})^2}{\sin(\frac{\delta_1}{2})^2}\right), \quad (15)$$

where the negative sign in front of the grating function in the last line of Eq. (15) stems from the identical negative weight in front of each source pair interference term in line 3 of Eq. (15), caused by the sum over all $(N-1)$ detectors being placed at the SP. The normalized Nth-order intensity correlation function, finally, reads

$$g^{(N)}_{N\mathrm{TLS}}(\delta_1, \mathrm{SP}) = 2 - \frac{1}{N^2} \frac{\sin(\frac{N\delta_1}{2})^2}{\sin(\frac{\delta_1}{2})^2}, \quad (16)$$

displaying an inverted grating function identical to the one obtained for quantum sources in Eq. (4), i.e., a subradiant intensity distribution $I_{|A_N\rangle}(\delta_1)$ produced by MSPEs and MPSs in the totally antisymmetric state $|A_N\rangle$. Note that, owing to the different constant term, the visibility of the classical subradiant pattern of Eq. (16) equals $\mathcal{V}_{\mathrm{TLS}} = 1/3$, independent of the number of sources N.

To reach higher visibilities for classical sources, one could increase the number of fixed detectors, e.g., using multiples α of complete sets of $N-1$ detectors placed at the SP, i.e., $\alpha(N-1)$, $\alpha \in \mathbb{N}_+$. In this case, we obtain [52]

$$g^{(1+\alpha(N-1))}_{N\mathrm{TLS}}(\delta_1, \alpha \times \mathrm{SP}) \sim 1 + \alpha - \frac{\alpha}{N^2} \frac{\sin(\frac{N\delta_1}{2})^2}{\sin(\frac{\delta_1}{2})^2}, \quad (17)$$

where in the limit $\alpha \gg 1$ the visibility $\mathcal{V}^{(\alpha)}_{\mathrm{TLS}} = \alpha/(\alpha+2)$ approaches unity, as in the case of quantum sources.

Note that an isomorphism between $G^{(m)}_{\rho_N}$ and $G^{(1)}_{\tilde{\rho}^{(m-1)}_N}$, where $m \in \mathbb{N}_+$, was recently identified for a light field ρ_N produced by N sources [15,16], i.e.,

$$G^{(m)}_{\rho_N}(\delta_1, \ldots, \delta_m) = G^{(1)}_{\tilde{\rho}^{(m-1)}_N}(\delta_1) G^{(m-1)}_{\rho_N}(\delta_2, \ldots, \delta_m), \quad (18)$$

where $\tilde{\rho}^{(m-1)}_N$ describes the state of the field after $m-1$ photons have been recorded at positions $\delta_2, \ldots, \delta_m$. In the case of N TLS and $\alpha(N-1)$ detectors placed at the SP, the projected state $\tilde{\rho}^{(\alpha(N-1))}_{N\mathrm{TLS}}$ reads

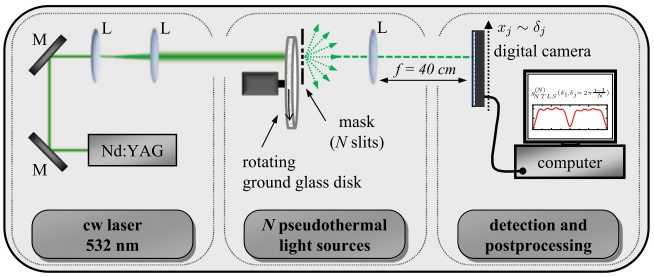

FIG. 2. Experimental setup to measure $g^{(N)}_{N\mathrm{TLS}}$ with N pseudothermal light sources. M, mirror; L, lens. For details, see the text and Ref. [14].

$$\tilde{\rho}^{(\alpha(N-1))}_{N\mathrm{TLS}} = \frac{[\prod_{j=2}^{N} E^{(+)}(\delta_j)]^{\alpha} \rho_{N\mathrm{TLS}} [\prod_{j=2}^{N} E^{(-)}(\delta_j)]^{\alpha}}{G^{(\alpha(N-1))}_{\rho_{N\mathrm{TLS}}}(\alpha \times \mathrm{SP})}, \quad (19)$$

with $\mathrm{Tr}[\tilde{\rho}^{(\alpha(N-1))}_{N\mathrm{TLS}}] = 1$. The state $\tilde{\rho}^{(\alpha(N-1))}_{N\mathrm{TLS}}$ is not of diagonal form, where the nondiagonal terms describe the correlations between the TLS induced by the detection of $\alpha(N-1)$ photons at the SP. The corresponding cross-correlation coefficient is given by [52]

$$\frac{\langle \hat{a}^{\dagger}_{l_1} \hat{a}_{l_2} \rangle_{\tilde{\rho}^{(\alpha(N-1))}_{N\mathrm{TLS}}}}{\sqrt{\langle \hat{a}^{\dagger}_{l_1} \hat{a}_{l_1} \rangle_{\tilde{\rho}^{(\alpha(N-1))}_{N\mathrm{TLS}}} \langle \hat{a}^{\dagger}_{l_2} \hat{a}_{l_2} \rangle_{\tilde{\rho}^{(\alpha(N-1))}_{N\mathrm{TLS}}}}} = -\frac{\alpha}{N + N\alpha - \alpha}, \quad (20)$$

demonstrating that the cross-correlations are negative and identical for any two sources where $l_1 \neq l_2$. Equation (20) shows that any state described by Eq. (19) displays destructive interference for all possible source pair combinations and thus will exhibit directional subradiance. Specifically, for $\alpha \gg N$, Eq. (20) becomes identical to Eq. (5), displaying the correlations between any two of the N multilevel atoms prepared in the totally antisymmetric state $|A_N\rangle$.

To measure $g^{(N)}_{N\mathrm{TLS}}$ for N statistically independent TLS, we use the pseudothermal light of a coherently illuminated rotating ground glass disk [54] (coherence time, $\tau_c \approx 50$ ms), impinging on a mask with N identical slits of width $a = 25$ μm and separation $d = 200$ μm (see Fig. 2). As a coherent light source, we utilize a linearly polarized frequency-doubled Nd:YAG laser at $\lambda = 532$ nm. Working in the high intensity regime, we employ a conventional digital camera placed in the far field of the mask to determine $g^{(N)}_{N\mathrm{TLS}}(\delta_1, \ldots, \delta_N)$, where we correlate $N-1$ pixels of the camera located at the SP $\sim \delta_2, \ldots, \delta_N$ with one moving pixel $\sim \delta_1$ (integration time of the camera, $\tau_i \approx 1$ ms $\ll \tau_c$) [14].

The experimental results for $g^{(N)}_{N\mathrm{TLS}}(\delta_1, \ldots, \delta_N)$ obtained in this way for $N = 2, \ldots, 5$ TLS are shown in Fig. 3. From the plots, the directional Dicke subradiant behavior of the N TLS is clearly visible, with dips of vanishing radiation that are in excellent agreement in position, depth, and width with the theoretical predictions of Eq. (16). This confirms

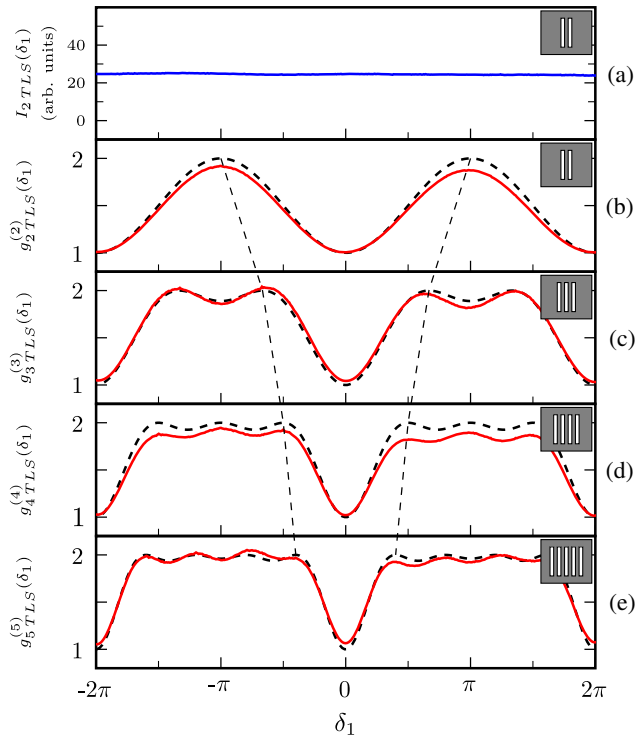

FIG. 3. Experimental results. (a) Average intensity $I_{2\mathrm{TLS}}(\delta_1)$ of $N = 2$ TLS demonstrating that the pseudothermal light sources are spatially incoherent in first order. (b)–(e) Measurement of the normalized Nth-order correlation function $g^{(N)}_{N\mathrm{TLS}}(\delta_1,\delta_j = 2\pi[(j-1)/N]; j = 2,\ldots,N) = \mathrm{G}^{(N)}_{N\mathrm{TLS}}(\delta_1,\delta_j = 2\pi[(j-1)/N]; j = 2,\ldots,N)/[I_{N\mathrm{TLS}}(\delta_1)\prod_{j=2}^{N} I_{N\mathrm{TLS}}(\delta_j = 2\pi[(j-1)/N])]$ for $N = 2,\ldots,5$ as a function of the first detector at δ_1 (the red solid curves). The suppression of incoherently emitted radiation at $\delta_1 = 0$ after $N-1$ photons have been recorded at the SP at $\delta_j = 2\pi[(j-1)/N]$, $j = 2,\ldots,N$, is clearly visible. The theoretical predictions of Eq. (16) are displayed by the black (dashed) curves.

the theory outlined above stating that (a) with distant quantum sources as well as classical TLS in corresponding states, directional subradiance can be observed [see Eqs. (4) and (17)], and that (b) directional subradiance of TLS occurs due to the similarity between the totally antisymmetric state $|A_N\rangle$ of N quantum sources and the highly correlated state $\tilde{\rho}^{(\alpha(N-1))}_{N\mathrm{TLS}}$, obtained from N initially uncorrelated TLS via $\alpha(N-1)$ photon detection events at the SP [see Eqs. (1) and (19)], leading to identical cross-correlations for N quantum sources and for N TLS in the limit $\alpha \gg N$ [see Eqs. (5) and (20)].

In conclusion, we discussed in this Letter the spatial aspects of Dicke subradiance, i.e., the emission profiles observed for incoherently emitting distant light sources prepared in totally antisymmetric states. We examined the conditions to achieve totally antisymmetric states for multilevel atoms, as well as multiphoton sources, and derived analytical expressions for the resulting spatial spontaneous emission patterns. We also showed that directional Dicke subradiance can be observed with incoherently emitting TLS, i.e., by measuring higher-order photon correlations projecting the TLS into highly correlated states. The latter result is unexpected, as subradiance is usually considered to be a nonclassical phenomenon displayed uniquely by quantum sources [48]. Directed emission of spontaneous emission has lately been discussed in the context of quantum communication and the coupling of quantum nodes within quantum networks [17–23], and more recently in the field of chiral quantum optics [24–27] and many-body subradiance [55–57]. The above analysis of directional Dicke subradiance could invoke new aspects in that framework, e.g., for chiral quantum optics in free space [58].

The authors thank G. S. Agarwal and S. Mährlein for the helpful comments and fruitful discussions. The authors gratefully acknowledge funding from the Erlangen Graduate School in Advanced Optical Technologies (SAOT) through the German Research Foundation (DFG) in the framework of the German excellence initiative. D. B. gratefully acknowledges the financial support from the Cusanuswerk, Bischöfliche Studienförderung.

*Corresponding author.
daniel.bhatti@fau.de

[1] R. H. Dicke, Phys. Rev. **93**, 99 (1954).
[2] N. E. Rehler and J. H. Eberly, Phys. Rev. A **3**, 1735 (1971).
[3] R. Friedberg, S. Hartmann, and J. Manassah, Phys. Rep. **7**, 101 (1973).
[4] G. S. Agarwal, *Quantum Optics*, Springer Tracts in Modern Physics Vol. 70 (Springer, Berlin, 1974).
[5] M. Gross and S. Haroche, Phys. Rep. **93**, 301 (1982).
[6] M. O. Scully, E. S. Fry, C. H. Raymond Ooi, and K. Wódkiewicz, Phys. Rev. Lett. **96**, 010501 (2006).
[7] M. O. Scully, Laser Phys. **17**, 635 (2007).
[8] M. O. Scully and A. A. Svidzinsky, Science **325**, 1510 (2009).
[9] T. Bienaimé, N. Piovella, and R. Kaiser, Phys. Rev. Lett. **108**, 123602 (2012).
[10] T. Bienaimé, R. Bachelard, N. Piovella, and R. Kaiser, Fortschr. Phys. **61**, 377 (2013).
[11] C. Navarrete-Benlloch, I. de Vega, D. Porras, and J. I. Cirac, New J. Phys. **13**, 023024 (2011).
[12] R. Röhlsberger, K. Schlage, B. Sahoo, S. Couet, and R. Rüffer, Science **328**, 1248 (2010).
[13] R. Wiegner, J. von Zanthier, and G. S. Agarwal, Phys. Rev. A **84**, 023805 (2011).
[14] S. Oppel, R. Wiegner, G. S. Agarwal, and J. von Zanthier, Phys. Rev. Lett. **113**, 263606 (2014).
[15] R. Wiegner, S. Oppel, D. Bhatti, J. von Zanthier, and G. S. Agarwal, Phys. Rev. A **92**, 033832 (2015).
[16] D. Bhatti, S. Oppel, R. Wiegner, G. S. Agarwal, and J. von Zanthier, Phys. Rev. A **94**, 013810 (2016).
[17] L.-M. Duan, M. D. Lukin, J. I. Cirac, and P. Zoller, Nature (London) **414**, 413 (2001).

[18] J. Simon, H. Tanji, J. K. Thompson, and V. Vuletić, Phys. Rev. Lett. **98**, 183601 (2007).
[19] H. J. Kimble, Nature (London) **453**, 1023 (2008).
[20] A. I. Lvovsky, B. C. Sanders, and W. Tittel, Nat. Photonics **3**, 706 (2009).
[21] X.-H. Bao, A. Reingruber, P. Dietrich, J. Rui, A. Dück, T. Strassel, L. Li, N.-L. Liu, B. Zhao, and J.-W. Pan, Nat. Phys. **8**, 517 (2012).
[22] E. Bimbard, R. Boddeda, N. Vitrant, A. Grankin, V. Parigi, J. Stanojevic, A. Ourjoumtsev, and P. Grangier, Phys. Rev. Lett. **112**, 033601 (2014).
[23] N. Maring, P. Farrera, K. Kutluer, M. Mazzera, G. Heinze, and H. de Riedmatten, Nature (London) **551**, 485 (2017).
[24] I. Söllner, S. Mahmoodian, S. L. Hansen, L. Midolo, A. Javadi, G. Kiršanskė, T. Pregnolato, H. El-Ella, E. H. Lee, J. D. Song, S. Stobbe, and P. Lodahl, Nat. Nanotechnol. **10**, 775 (2015).
[25] C. Sayrin, C. Junge, R. Mitsch, B. Albrecht, D. O'Shea, P. Schneeweiss, J. Volz, and A. Rauschenbeutel, Phys. Rev. X **5**, 041036 (2015).
[26] S. Rosenblum, O. Bechler, I. Shomroni, Y. Lovsky, G. Guendelman, and B. Dayan, Nat. Photonics **10**, 19 (2016).
[27] P. Lodahl, S. Mahmoodian, S. Stobbe, A. Rauschenbeutel, P. Schneeweiss, J. Volz, H. Pichler, and P. Zoller, Nature (London) **541**, 473 (2017).
[28] D. Pavolini, A. Crubellier, P. Pillet, L. Cabaret, and S. Liberman, Phys. Rev. Lett. **54**, 1917 (1985).
[29] R. G. DeVoe and R. G. Brewer, Phys. Rev. Lett. **76**, 2049 (1996).
[30] C. Hettich, C. Schmitt, J. Zitzmann, S. Kühn, I. Gerhardt, and V. Sandoghdar, Science **298**, 385 (2002).
[31] M. D. Barnes, P. S. Krstic, P. Kumar, A. Mehta, and J. C. Wells, Phys. Rev. B **71**, 241303 (2005).
[32] Y. Takasu, Y. Saito, Y. Takahashi, M. Borkowski, R. Ciuryło, and P. S. Julienne, Phys. Rev. Lett. **108**, 173002 (2012).
[33] B. H. McGuyer, M. McDonald, G. Z. Iwata, M. G. Tarallo, W. Skomorowski, R. Moszynski, and T. Zelevinsky, Nat. Phys. **11**, 32 (2015).
[34] V. V. Temnov and U. Woggon, Phys. Rev. Lett. **95**, 243602 (2005).
[35] P. A. Vetter, L. Wang, D.-W. Wang, and M. O. Scully, Phys. Scr. **91**, 023007 (2016).
[36] H. H. Jen, M.-S. Chang, and Y.-C. Chen, Phys. Rev. A **94**, 013803 (2016).
[37] A. Maser, U. Schilling, T. Bastin, E. Solano, C. Thiel, and J. von Zanthier, Phys. Rev. A **79**, 033833 (2009).
[38] C. Ammon, A. Maser, U. Schilling, T. Bastin, and J. von Zanthier, Phys. Rev. A **86**, 052308 (2012).
[39] D. Plankensteiner, L. Ostermann, H. Ritsch, and C. Genes, Sci. Rep. **5**, 16231 (2015).
[40] S.-Q. Tang, J.-B. Yuan, L.-M. Kuang, and X.-W. Wang, Quantum Inf. Process. **14**, 2883 (2015).
[41] M. O. Scully, Phys. Rev. Lett. **115**, 243602 (2015).
[42] I. M. Mirza and T. Begzjav, Europhys. Lett. **114**, 24004 (2016).
[43] A. Canaguier-Durand and R. Carminati, Phys. Rev. A **93**, 033836 (2016).
[44] F. Damanet, D. Braun, and J. Martin, Phys. Rev. A **94**, 033838 (2016).
[45] R. J. Bettles, S. A. Gardiner, and C. S. Adams, Phys. Rev. A **94**, 043844 (2016).
[46] R. Ganesh, L. Theerthagiri, and G. Baskaran, Phys. Rev. A **96**, 033829 (2017).
[47] H. H. Jen, Phys. Rev. A **96**, 023814 (2017).
[48] M. Hebenstreit, B. Kraus, L. Ostermann, and H. Ritsch, Phys. Rev. Lett. **118**, 143602 (2017).
[49] W. Guerin and R. Kaiser, Phys. Rev. A **95**, 053865 (2017).
[50] W. Guerin, M. O. Araújo, and R. Kaiser, Phys. Rev. Lett. **116**, 083601 (2016).
[51] P. Chowdhury, T. Pramanik, A. S. Majumdar, and G. S. Agarwal, Phys. Rev. A **89**, 012104 (2014).
[52] See Supplemental Material at http://link.aps.org/supplemental/10.1103/PhysRevLett.120.113603 for detailed calculations.
[53] R. J. Glauber, Phys. Rev. **130**, 2529 (1963).
[54] L. E. Estes, L. M. Narducci, and R. A. Tuft, J. Opt. Soc. Am. **61**, 1301 (1971).
[55] G. Facchinetti, S. D. Jenkins, and J. Ruostekoski, Phys. Rev. Lett. **117**, 243601 (2016).
[56] S. D. Jenkins, J. Ruostekoski, N. Papasimakis, S. Savo, and N. I. Zheludev, Phys. Rev. Lett. **119**, 053901 (2017).
[57] A. Asenjo-Garcia, M. Moreno-Cardoner, A. Albrecht, H. J. Kimble, and D. E. Chang, Phys. Rev. X **7**, 031024 (2017).
[58] A. Grankin, D. V. Vasilyev, P. O. Guimond, B. Vermersch, and P. Zoller, arXiv:1802.05592.